Supporting Information

Water-enhancement in CO_2 Capture by Amines: An Insight into CO_2-H_2O Interactions on Amine Films and Sorbents

Jie Yu[1†], Yuxin Zhai[1†], and Steven S.C. Chuang[1]*

[1] Department of Polymer Science, the University of Akron, 170 University Avenue, Ohio 44325, United States

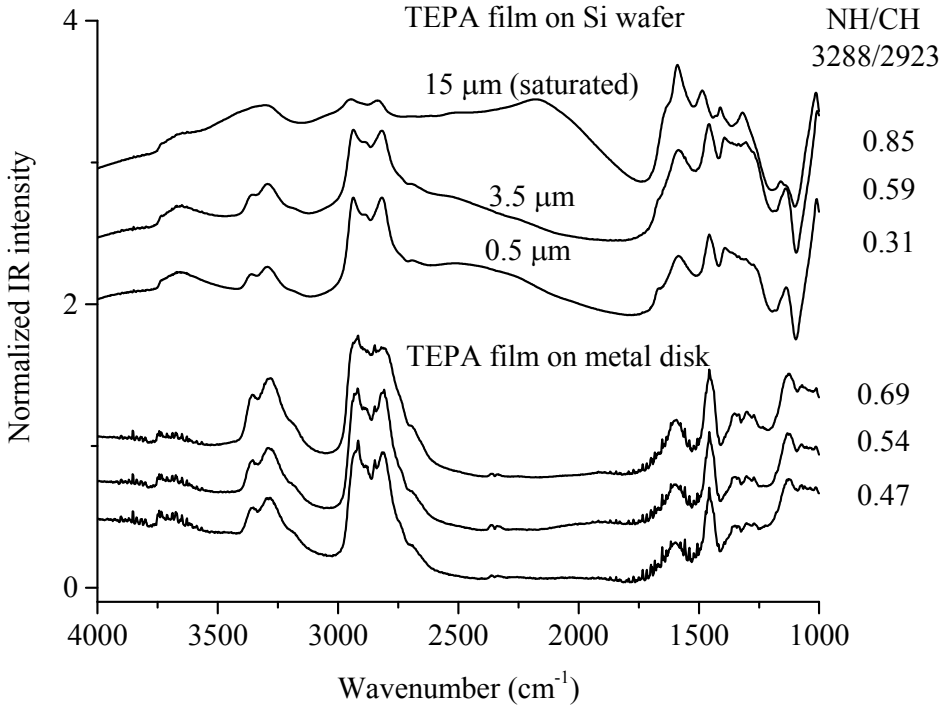

Figure S1. Comparison of IR absorbance spectra of TEPA films on the stainless steel disk and Si wafer.

The IR intensity ratio of TEPA films on Si wafer was correlated with the that of TEPA films on stainless steel disk to determine the thickness.

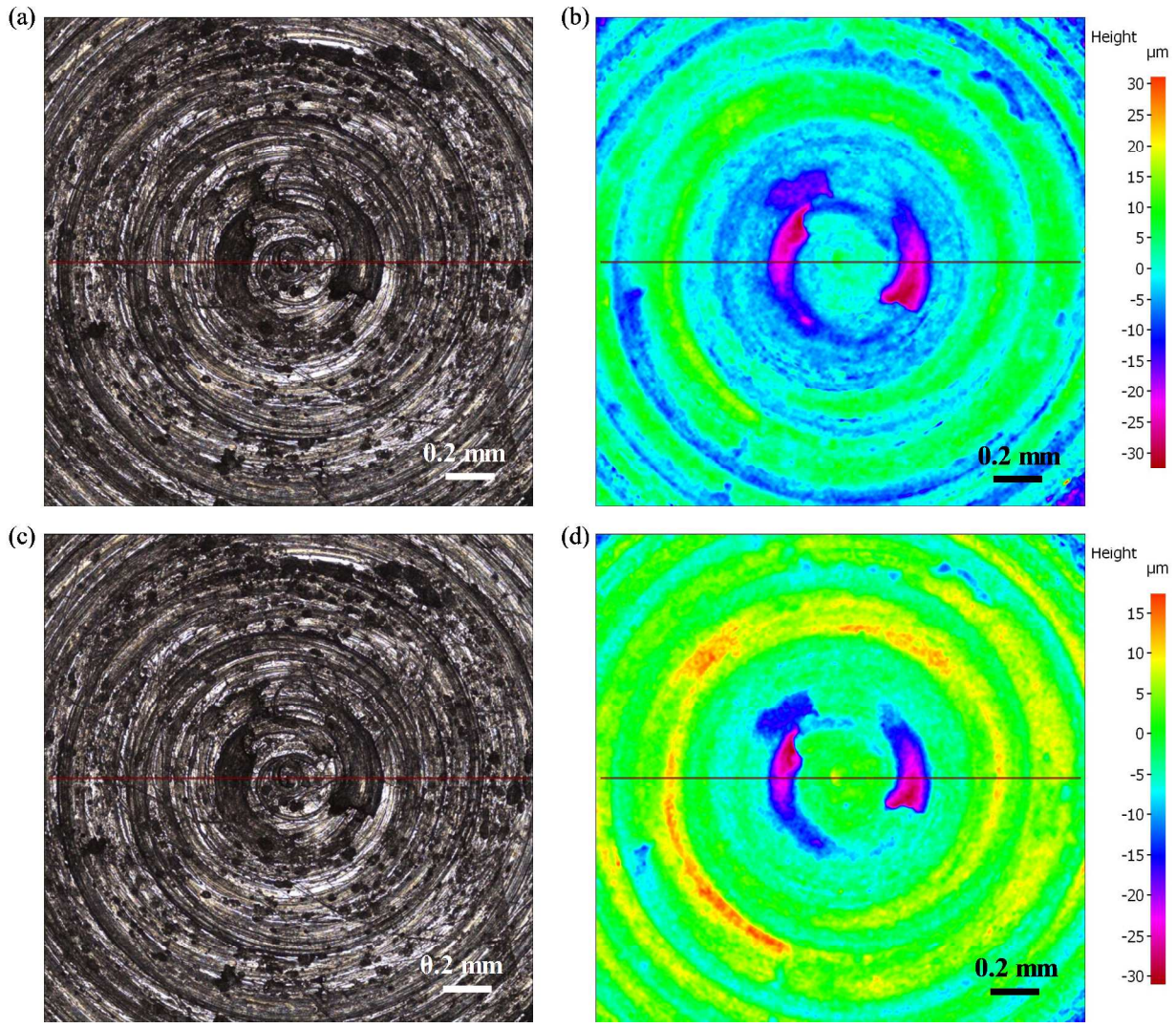

Figure S2. (a) Optical microscope and (b) the profile of surface roughness of the stainless steel disk. (c) Optical microscope and (d) the profile of surface roughness of 0.8 µm TEPA film on stainless steel disk. The images were taken by InfiniteFocus.

Table S1. Surface roughness of the stainless steel and 0.8 µm TEPA film on stainless steel disk.

	Stainless steel disk (µm)	0.8 µm TEPA on stainless steel disk
Ra (roughness average)	1.6621	1.6849
Rq (root mean square roughness)	2.1279	2.0686

The roughness of the stainless steel disk is similar as that of the 0.8 µm TEPA film on the stainless steel disk

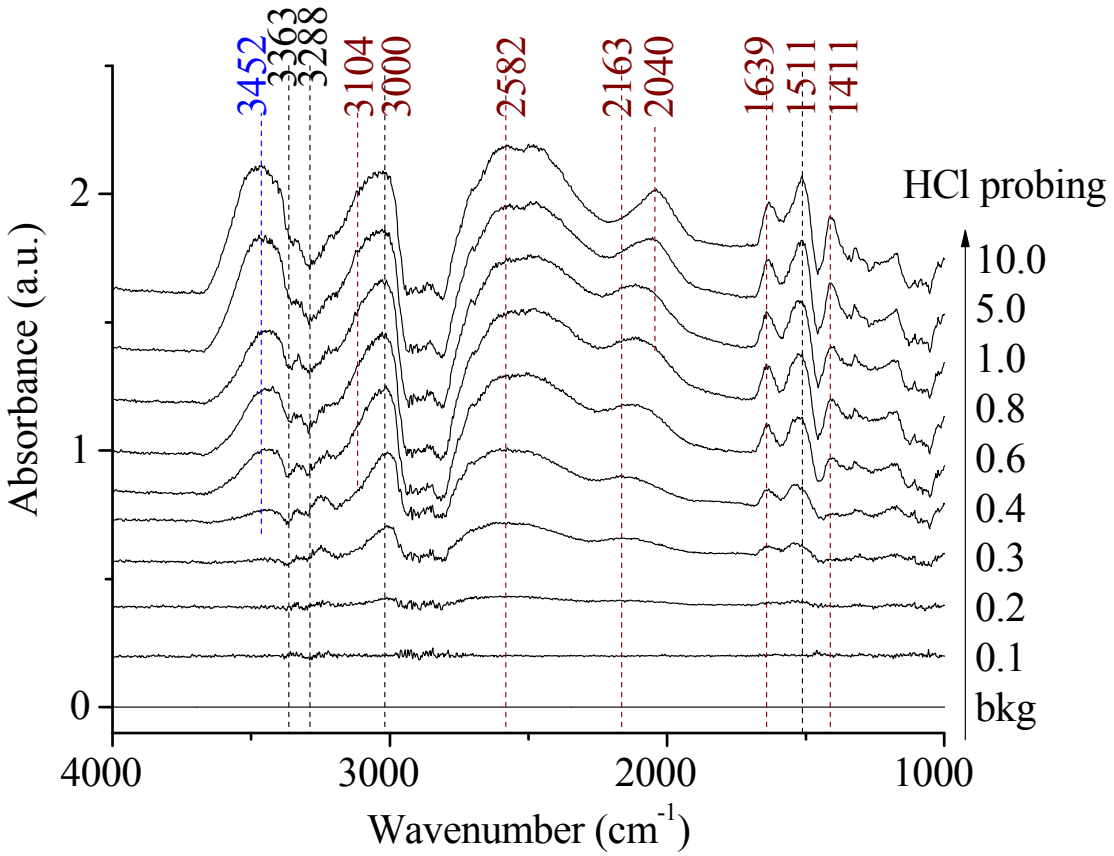

Figure S3. IR absorbance spectra of 10 μm TEPA film during HCl probing. IR absorbance spectra were obtained by subtracting the spectra after pretreatment.

Flowing HCl/H_2O on TEPA film produced ammonium ions from 0 to 0.3 min and ammonium ions – water hydrogen bonding after 0.3 min. All of the bands produced during 0 – 0.3 min can be attributed ammonium ions. The IR bands of ammonium ions could be ambiguously assigned from **Figure S3**.

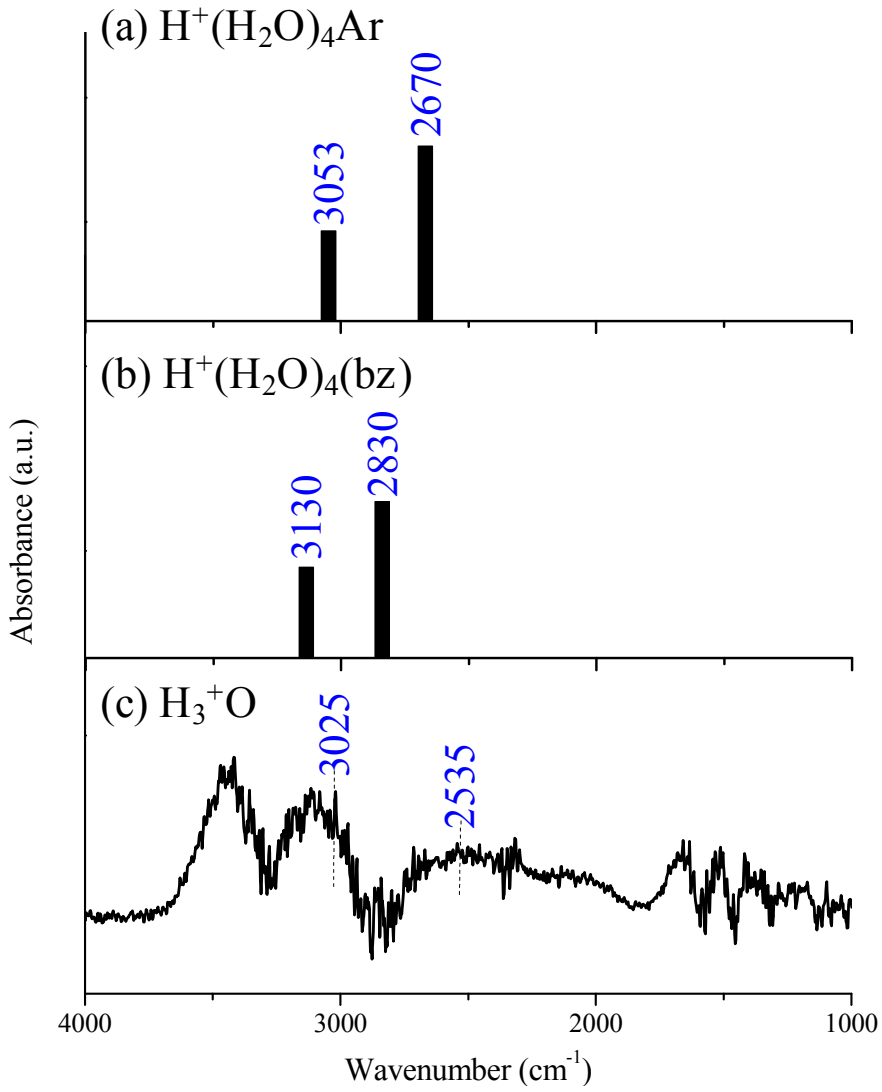

Figure S4. IR absorbance spectra of (a) $H^+(H_2O)_4(Ar)$, (b) $H^+(H_2O)_4(bz)$ and (c) H_3O^+.[1] The IR spectrum in (c) was obtained by $I_{0.3\ min} - I_{0.2\ min}$ at CO_2/H_2O adsorption on 10 μm TEPA film, shown in Figure 4 inset.

Figure S4 (a) and (b) showed that clusters of hydronium ions gave peaks in the region of 3000 – 3200 cm^{-1} and 2500 – 2900 cm^{-1}, which were consistent with CO_2/H_2O adsorption on TEPA film in **Figure S4** (c).

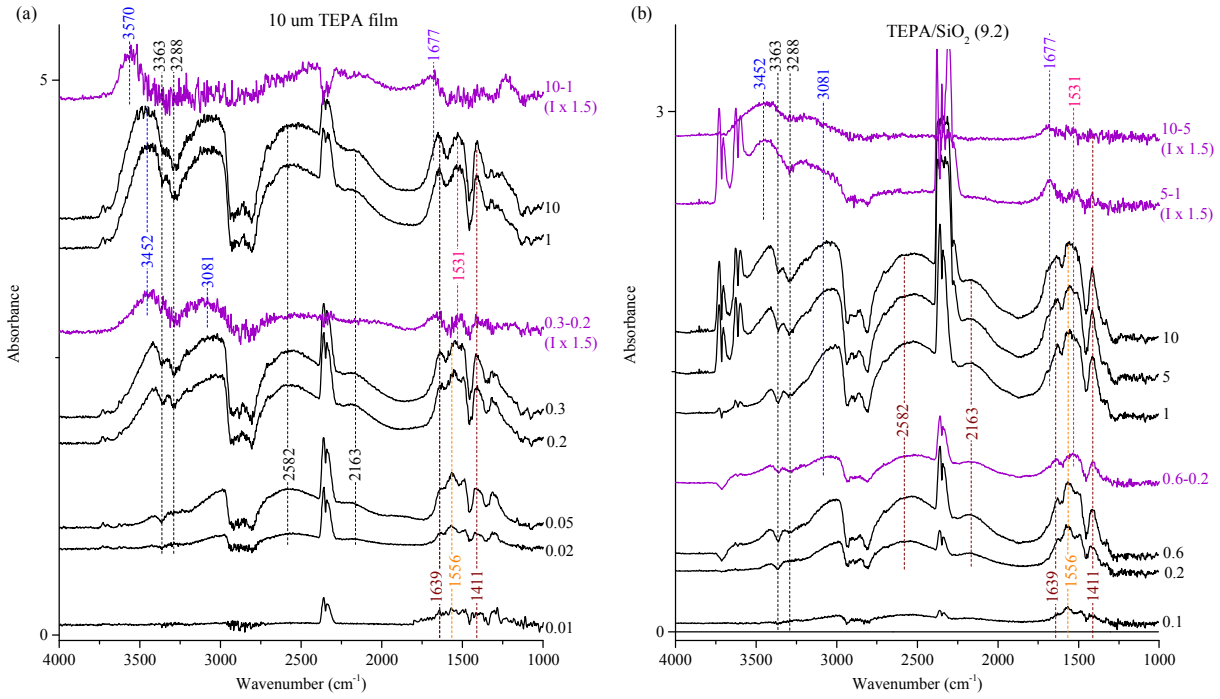

Figure S5. IR absorbance spectra of (a) 10 μm TEPA film and (b) TEPA/SiO_2 (9.2) during CO_2/H_2O adsorption. Insets are the difference spectra of adsorbed species on 10 μm TEPA film during CO_2/H_2O adsorption.

Adsorbed CO_2 on both 10 μm TEPA film in **Figure S5** (a) and TEPA/SiO_2 (9.2) in **Figure S5** (b) show similar IR features during CO_2/H_2O adsorption, indicating both TEPA film and sorbent followed a same pathway.

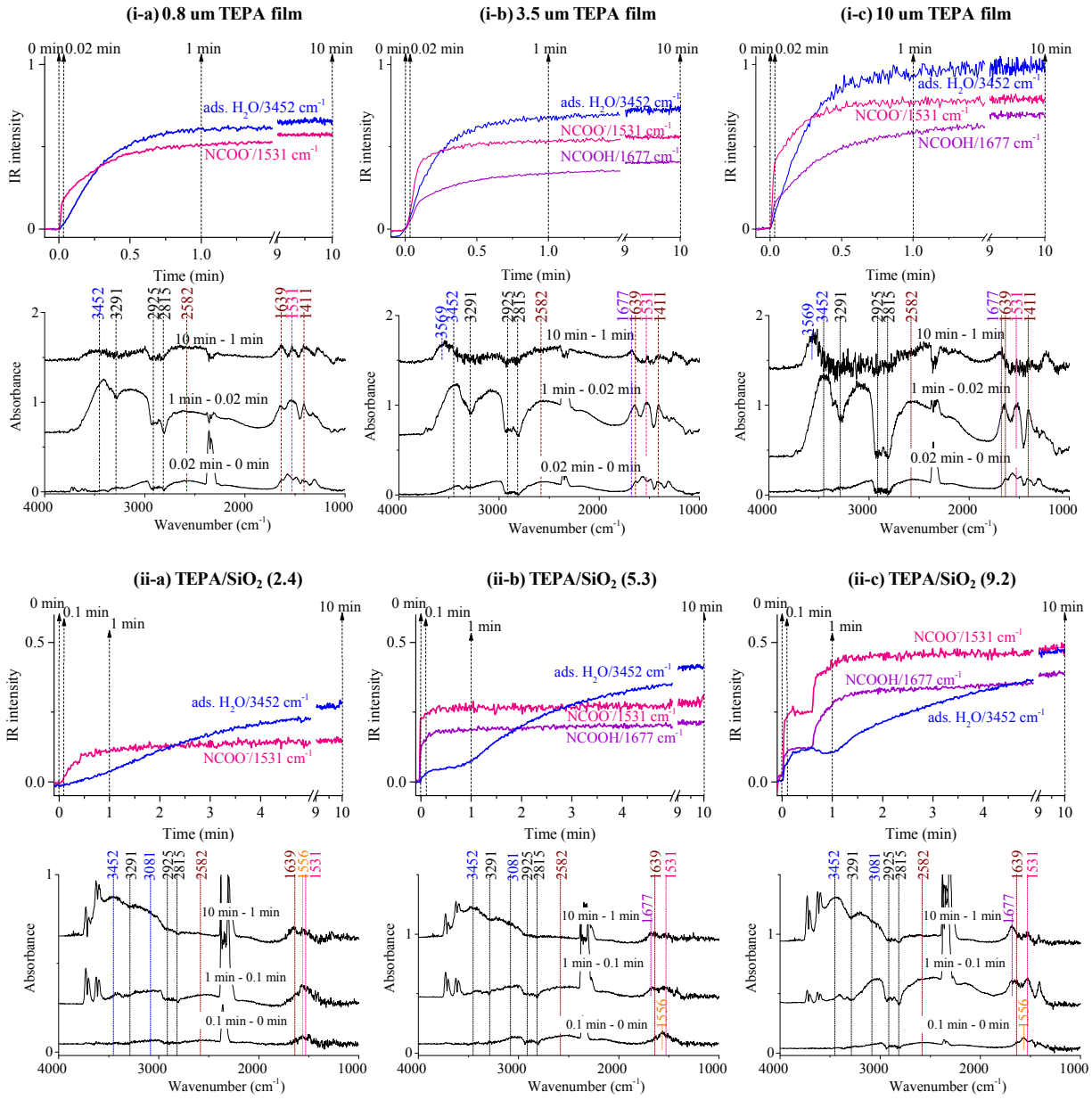

Figure S6. IR intensity profiles and IR absorbance spectra of TEPA films and TEPA/SiO_2 sorbents during CO_2/H_2O adsorption for 10 min.

Adsorbed CO_2 on both 10 μm TEPA film in **Figure S6** (a) and TEPA/SiO_2 (9.2) in **Figure S6** (b) show similar IR features during CO_2/H_2O adsorption, suggesting the density of the amine functional groups and their states are nearly identical.

Determining the molar absorption coefficients of adsorbed CO_2 on TEPA films

Beer's law gives the absorbance $A = \varepsilon lc$, where c is the molar concentration of species in the material, l is the path length of the beam, and ε is the molar absorption coefficient.[2] In this study, we assumed (i) the TEPA films were homogeneously distributed on metal disk, (ii) IR beam could penetrate the TEPA films, and (iii) IR beam reflects once in TEPA films (no diffuse reflectance). The molar concentration of adsorbed CO_2 was obtained from the CO_2 capture capacity of TEPA films. The path length of TEPA films were calculated followed a previous work.[3] The molar absorption coefficient of ammonium carbamate at 2561 cm^{-1}, corresponding to the value of slope of calibration curves in **Figure S7 (c)**, was determined to be 0.02546 L $(mmol\ cm)^{-1}$ with 8% of error. The thickness of each layer was estimated using $A = \varepsilon lc$ with ε=0.02546 L $(mmol\ cm)^{-1}$, A = the intensity of 2561 cm^{-1} at specific thickness, and c = total molar concentration of adsorbed CO_2 at specific thickness.

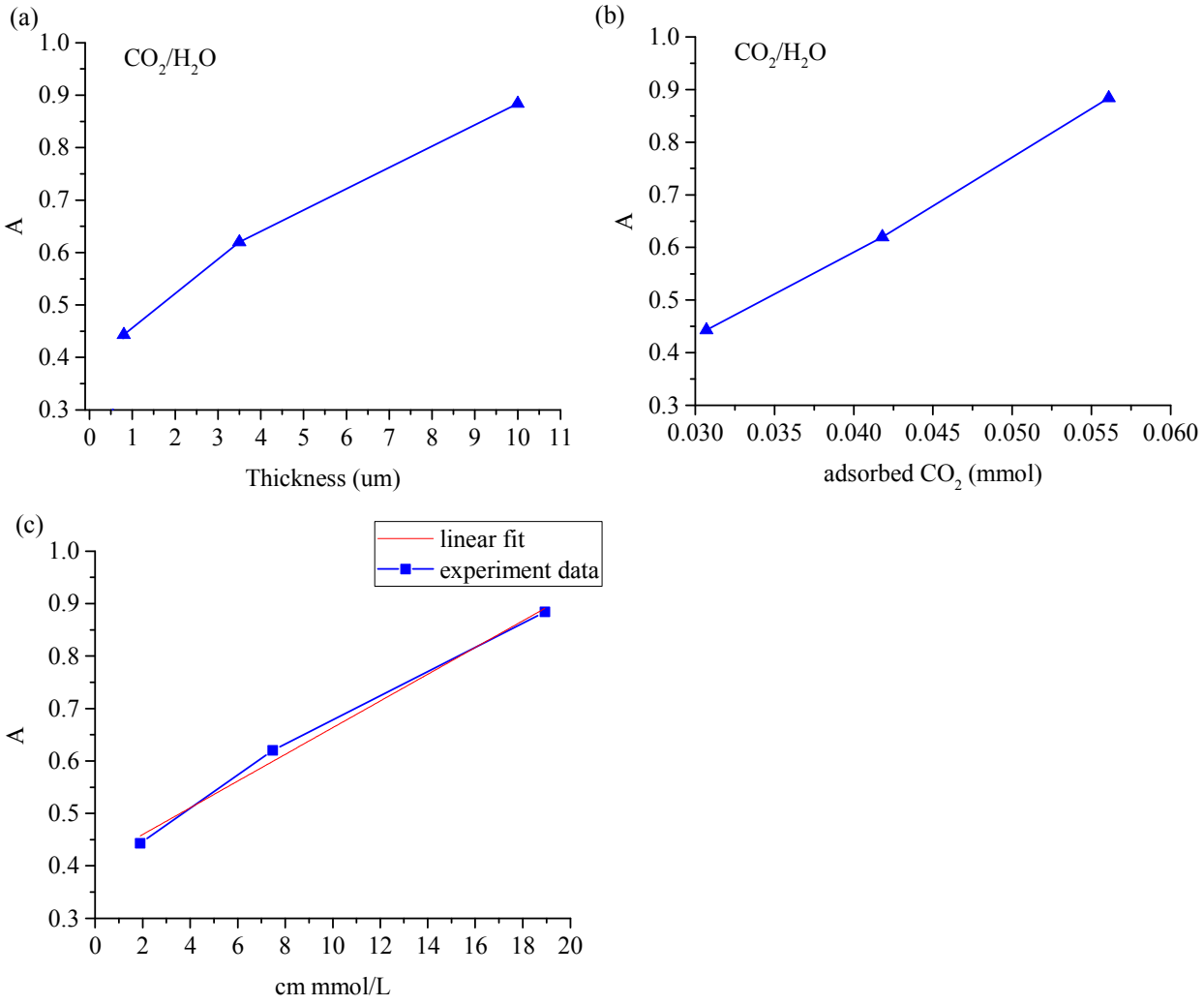

Figure S7. Relationship between IR intensity at 2561 cm^{-1} (A) and (a) thickness, (b) adsorbed CO_2, and (c) path length × concentration of adsorbed CO_2.

The thickness of top, middle, and bottom layers of TEPA films was determined by the IR intensity of ammonium carbamate at 2561 cm^{-1}, which increased linearly with the thickness of TEPA films (**Figure S7 (a)**). The IR intensity obtained from IR absorbance spectra of 0.02, 1, and 10 min and IR difference spectra of 1-0.02 and 10-1 min could be fitted in **Figure S7 (a)** and correlate with the thickness of each layer, shown in **Table S2**.

Table S2. Calibration of thickness by ammonium carbamate at 2561 cm^{-1}

Ads. time (min)	IR intensity at 2561 cm^{-1}			Calibrated thickness (μm)*		
	0.8 μm	3.5 μm	10 μm	0.8 μm	3.5 μm	10 μm
0.02 (top layer)	0.123	0.144	0.135	0.2-0.3	0.3-0.4	0.3-0.4
1	0.375	0.552	0.787	0.7-0.8	2.5-2.7	7.5-7.7
1-0.02 (middle layer)	0.252	0.408	0.652	0.5-0.6	0.9-0.1.2	4.3-4.5
10	0.443	0.620	0.883	0.8	3.5	10
10-1 (bottom layer)	0.068	0.068	0.097	0.1-0.2	0.1-0.2	0.1-0.2

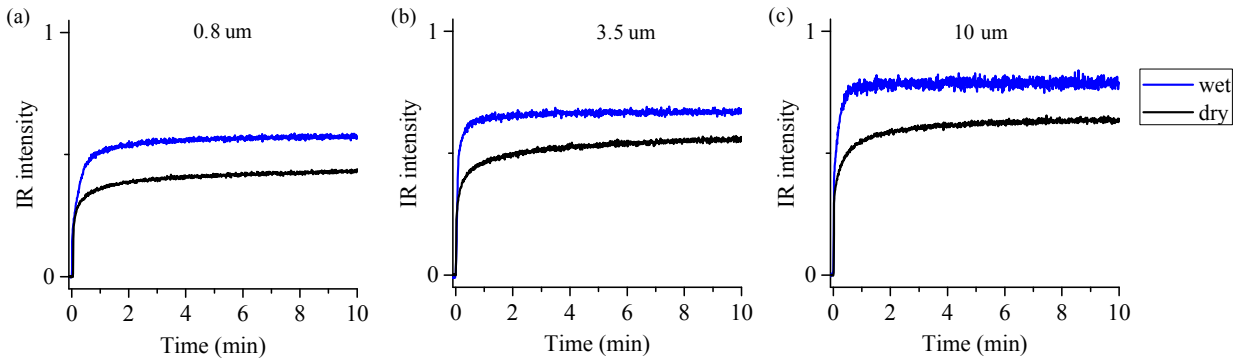

Figure S8. IR intensity profiles of adsorbed species at 1531 cm^{-1} during wet and dry CO_2 adsorption on (a) 0.8, (b) 3.5, and (c) 10 μm TEPA films.

Figure S8 shows a sharp rise and the immediate level-off of carbamate profile during dry CO_2 adsorption on TEPA films. Adding H_2O in CO_2 stream showed higher intensity of adsorbed CO_2 at 1531 cm^{-1} ($-NCOO^-$), indicating the enhancement of CO_2 capture capacity on TEPA films. Adsorption halftimes ($t_{1/2}$) were obtained from the above curves and listed in **Table 1** for comparison of adsorption kinetics.

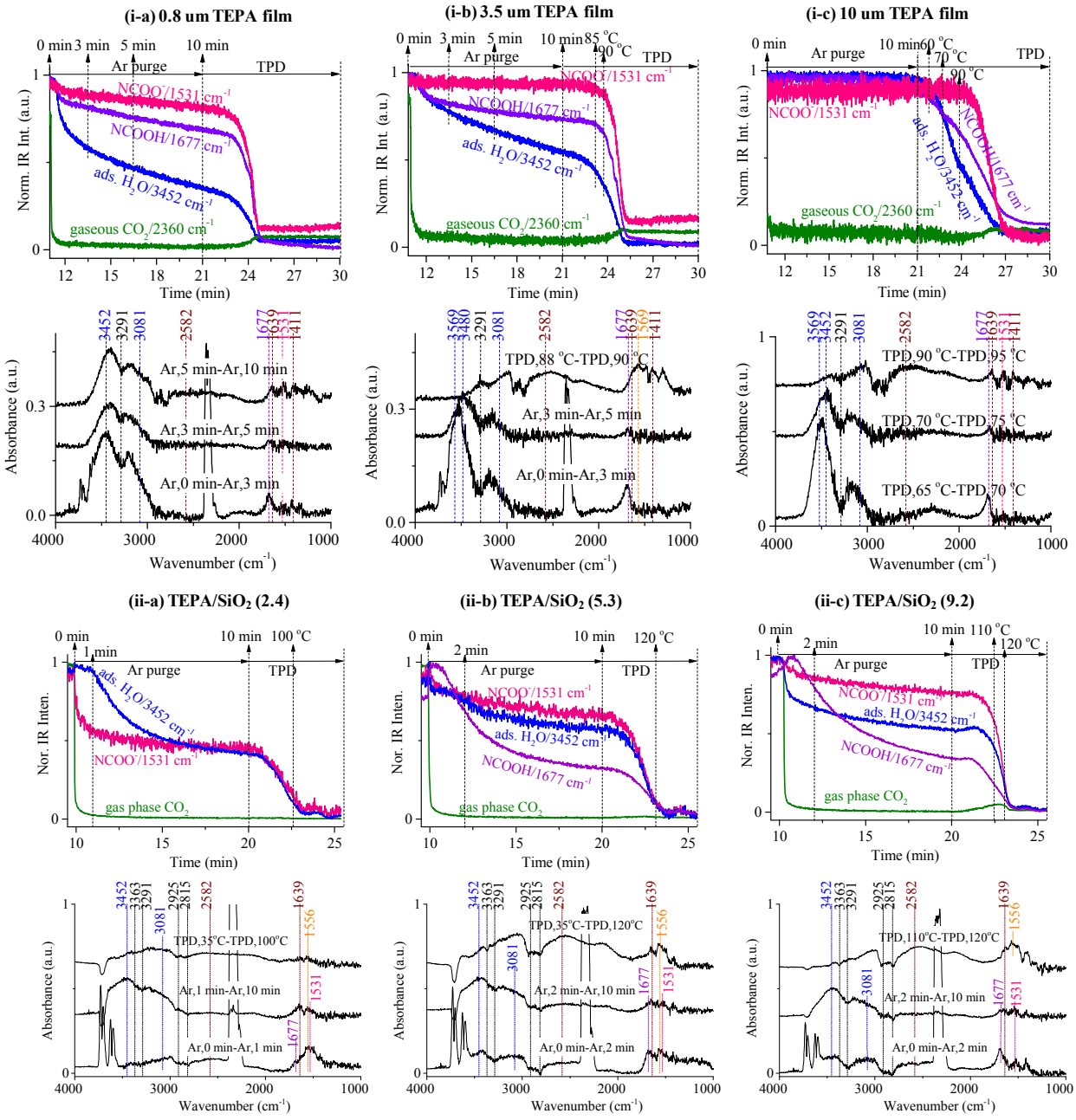

Figure S9. Normalized IR intensity profiles and IR absorbance spectra of TEPA films and TEPA/SiO_2 sorbents during Ar purging and TPD after exposure to CO_2/H_2O flow for 10 min.

The desorption of adsorbed species from TEPA/SiO_2 in **Figure S9** followed the same trend as TEPA films but gave low desorption temperatures. This observation suggests the amine density on SiO_2 support is lower than those of amine thin films.

Table S3. CO_2 capture capacity and amine efficiency of TEPA films under various modes of H_2O exposures.[4]

Liquid film*	CO_2 concentration	H_2O content	Capture Capacity* (mmol/g)	Amine eff.*
TEPA	15 vol%	3 wt%	8.98	0.34
TEPA	15 vol%	1 wt%	9.29	0.41
TEPA	15 vol%	0.5 wt%	5.67	0.25
mixed TEPA/H_2O	15 vol%	16.7 wt%	14.38	0.54
mixed TEPA/H_2O	15 vol%	8.3 wt%	6.76	0.30
mixed TEPA/H_2O	15 vol%	4.8 wt%	2.52	0.11

*The thickness of TEPA film in previous paper was theoretically calculated as 20 μm. The same TEPA film was calibrated in this paper with the thickness of 10 μm.

References

1. Cheng, T. C.; Bandyopadhyay, B.; Mosley, J. D.; Duncan, M. A., IR Spectroscopy of Protonation in Benzene–Water Nanoclusters: Hydronium, Zundel, and Eigen at a Hydrophobic Interface. *J. Am. Chem. Soc.* **2012,** *134* (31), 13046-13055.
2. Griffiths, P. R.; De Haseth, J. A., Fourier Transform Infrared Spectroscopy, Second Edition; John Wiley & Sons, Inc.: Hoboken, NJ, 2007; pp 1-529.
3. Wilfong, W. C.; Srikanth, C. S.; Chuang, S. S. C., In Situ ATR and DRIFTS Studies of the Nature of Adsorbed CO_2 on Tetraethylenepentamine Films. *ACS Appl. Mater. Interfaces* **2014**, *6* (16), 13617-13626.
4. Yu, J.; Chuang, S. S. C., The Role of Water in CO_2 Capture by Amine. *Ind. Eng. Chem. Res.* **2017**, *56* (21), 6337-6347.